Available online at www.sciencedirect.com
ScienceDirect
Journal of Hazardous Materials 147 (2007) 1037–1050
Journal of Hazardous Materials
www.elsevier.com/locate/jhazmat

Total flammable mass and volume within a vapor cloud produced by a continuous fuel-gas or volatile liquid-fuel release

Michael Epstein *, Hans K. Fauske

Fauske & Associates, LLC, 16W070 West 83rd Street, Burr Ridge, IL 60527, United States

Received 24 July 2006; received in revised form 11 January 2007; accepted 26 January 2007
Available online 6 February 2007

Abstract

The top-hat jet/plume model has recently been employed to obtain simple closed-form expressions for the mass of fuel in the flammable region of a vapor "cloud" produced by an axisymmetric (round) continuous-turbulent jet having positive or negative buoyancy [1]. The fuel release may be a gas or a volatile liquid. In this paper, the top-hat analysis is extended to obtain closed-form approximate expressions for the total mass (fuel + entrained air) and volume of the flammable region of a release cloud produced by either a round or a plane (two-dimensional) buoyant jet. These expressions lead to predicted average fuel concentrations in the flammable regions of the release clouds which, when compared with the stoichiometric concentration, serve as indicators of the potential severity of release cloud explosions. For a fixed release mass, the combustion overpressure following ignition of a hydrogen/air cloud is anticipated to be significantly lower than that due to ignition of a hydrocarbon/air cloud. The predicted average hydrogen concentration within the flammable region of the release cloud is below the lower detonability limit. The facility with which the expressions can be used for predictions of combustion overpressures is illustrated for propane releases and deflagrations in a closed compartment.

Keywords: Fuel-gas release; Volatile liquid-fuel release; Jet; Plume; Flammable vapor cloud

1. Introduction

Accidental releases of liquid or gaseous fuel indoors or to the outside is a safety problem that is frequently considered by the chemical and waste remediation industries that process and/or store flammable substances. The release almost always occurs in the form of a negatively or positively buoyant, continuous jet which mixes with the ambient air. All possible fuel/ambient air mixture compositions occur within the buoyant jet between its source and the far field of the jet. Since these compositions pass through the flammable region, a combustible region is created. The ambient overpressure that could occur after ignition of the flammable region depends on the volume and/or mass of the flammable region.

Marshall [2] considered continuous fuel-gas releases and treated separately the cases of a momentum jet and a buoyant plume. Closed-form expressions for the volume and mass of flammable material were obtained by integrating available semi-empirical Gaussian-distribution formulas for the concentration profiles, as reviewed and recommended by Long [3] for a momentum jet and for a point source buoyant plume.

Epstein and Fauske [1] derived a closed-form expression for the mass of fuel-gas within the flammable region of a vertical, round jet formed by a continuous source of fuel-gas which incorporates the effects of release momentum, positive and negative release buoyancy, finite release area, and an inert carrier gas. They demonstrated that this expression with a numerically modified Froude number may also be used to predict the mass of fuel material in the flammable region of a volatile liquid-fuel release. The utility of the expression for liquid-fuels was tested by comparing its predictions with an available numerical model [4] of the dispersion of volatile liquid chemicals released from pressurized storage vessels. It was also shown in ref. [1] that the mass of fuel within the flammable region of a volatile liquid-fuel release directed horizontally or inclined from the horizontal by as much as 45° can be accurately estimated from a simple, purely momentum-controlled jet dilution model.

* Corresponding author. Tel.: +1 630 887 5210; fax: +1 630 986 5481.
E-mail address: Epstein@fauske.com (M. Epstein).

0304-3894/$ – see front matter © 2007 Elsevier B.V. All rights reserved.
doi:10.1016/j.jhazmat.2007.01.138

Nomenclature

$B(x)$	incomplete beta function defined by Eq. (46) for negatively buoyant round jets, Eq. (76) for negatively buoyant plane jets
c_f	liquid specific heat
C_D	flow orifice coefficient
E_0	entrainment coefficient ($\cong$0.1)
Fr	Froude number, Eq. (19) for positively buoyant round gas jet, Eq. (40) for negatively buoyant round gas and volatile liquid-fuel jets, Eq. (55) for positively buoyant plane gas jet, Eq. (73) for negatively buoyant plane gas and volatile liquid-fuel jets
Fr_{cr}	critical Froude number of negatively buoyant jet below which jet is not diluted below the LFL during jet rise to its maximum height
g	gravitational constant
G	release mass flux (kg m^{-2} s^{-1})
h	enthalpy
h_{fg}	latent heat of evaporation
I_{flam}	integral for flammable fuel mass given by Eq. (26) for positively buoyant round gas jet, Eq. (43) for negatively buoyant round gas jet, Eq. (52) for vertical round liquid-fuel jet, Eq. (65) for positively buoyant plane gas jet, Eq. (74) for negatively buoyant plane gas jet
$I_{flam,t}$	integral for total flammable gas given by Eq. (32) for positively buoyant round gas jet, Eq. (48) for negatively buoyant round gas jet, Eq. (53) for vertical round liquid-fuel jet, Eq. (66) for positively buoyant plane gas jet, Eq. (75) for negatively buoyant plane gas jet
L	lateral dimension of plane jet
m_{flam}	mass of flammable fuel material
$m_{flam,t}$	total flammable mass (fuel-gas + air)
N	Froude number correction factor for volatile liquid-fuel releases (0.62)
P	pressure
$\dot{Q}$	volumetric flow of light gas from a point or line source (m^3 s^{-1})
R	radius of round jet and half-width of plane jet
R_{id}	ideal gas constant
T	temperature
v	jet velocity
v_{fg}	change in specific volume due to evaporation
V_{flam}	volume of flammable region
x_0	vapor mass fraction (quality) in two-phase (liquid–vapor) depressurized jet
Y	fuel mass fraction
$\bar{Y}$	average fuel mass fraction ($m_{flam}/m_{flam,t}$)
Y_0	mass fraction of fuel-gas in a release containing inert gas (air)
z	distance from jet source

Greek letters

γ	ideal gas ratio of specific heats
λ	jet dilution factor, Eq. (17)
ξ	dummy integration variable
ρ	jet mixture density

Subscripts

a	refers to ambient conditions (or initial compartment atmosphere conditions)
bp	boiling point
e	refers to conditions at the vent exit plane
f	refers to saturated liquid in two-phase mixture
g	refers to saturated vapor in two-phase mixture
LFL	refers to lower flammability condition
0	refers to initial or equivalent source conditions
st	refers to stagnation conditions inside vessel
stoic	refers to the stoichiometric composition of the fuel/air mixture
UFL	refers to upper flammability condition

It is worth mentioning that the expression in ref. [1] for the mass of flammable fuel material in a vertical buoyant jet at atmospheric pressure was derived without appealing to the Boussinesq approximation in that density variations were allowed everywhere density appeared in the governing equations. This was accomplished by assuming isothermal flow and assigning top-hat profiles to plume properties. That is, at a given height z above the source the properties ρ, v and Y have one constant value inside the jet and another outside it (see "Nomenclature" for the meanings of the symbols). In a second paper on the subject, Epstein and Fauske [5] examined the validity of the top-hat model for predicting the flammable mass by comparing top-hat model predictions with those of a numerical Gaussian jet model that fully accounts for realistic radial profiles of jet properties. The numerical calculations confirmed the top-hat model for jet flammable mass calculations.

The closed-form expression that appears in ref. [1] predicts the mass of fuel material within the flammable region of a vertical buoyant jet. Estimation of the overpressure caused by ignition of the flammable region requires knowledge of the total mass (fuel + air) in the flammable region. One may close the problem using only the flammable fuel mass prediction by conservatively assuming that the entrained ambient air and fuel material in the flammable region have stoichiometric concentrations. Actually, the fuel/air mixture in the flammable region departs significantly from stoichiometry and it is desirable to account for this when making overpressure predictions.

Implicit to the previous analysis [1] are the desired relationships for the total mass (fuel + entrained air) and the volume of the flammable region within a round, continuous, buoyant fuel-gas or volatile liquid-fuel jet release in terms of definite integrals involving a dimensionless Froude number parameter. In this paper, these integrals are converted to approximate analytical forms that permit simplification in the computational procedure.

Also, expressions for the total mass and volume of the flammable region within a plane jet are obtained, to cover the case of slot-like leak openings, by simply following the mathematical steps for the round jet [1]. Useful by-products of the analyses are simple quantitative expressions for the average fuel concentrations in the flammable region of a release which provide a "feeling" for the magnitude of the pressure rise following the ignition of the release.

Before jet mixing and flammable regions are discussed it is necessary to consider the region just outside the jet release orifice where jet expansion and depressurization may occur and, therefore, when the equations of jet dilution do not apply.

2. The jet expansion region

In some breach of containment (vessel) problems the pressure inside the vessel is equal to the outside ambient pressure. The fuel-gas in the vessel flows out of the breach because it is lighter than air (e.g., H_2 fuel-gas). The density difference induces a buoyancy-driven, countercurrent flow of the light fuel-gas out of the vessel and room air into the vessel. Upon emerging from the vessel the light fuel-gas forms a turbulent, purely buoyant light fuel/entrained air plume. In this case the size of the flammable region within the plume may be estimated without consideration of a jet expansion region. This light fuel release problem is frequently encountered in safety analyses of waste storage facilities. In most vessel discharge scenarios, however, the release scenario involves a pressurized vessel or pipe of a gaseous or liquefied fuel substance.

If the release involves gaseous fuel and the pressure in the vessel or pipe (hereafter referred to as the stagnation pressure) is not too high the gas is fully depressurized at the breach exit plane and the source properties of the jet (v_0, ρ_0, R_0) coincide with those at the breach exit plane. However, as the stagnation pressure increases, a point is reached at the so-called critical pressure ratio when the exit velocity reaches the speed of sound. At higher stagnation pressures, the exit velocity remains locally sonic, but the exit pressure rises above ambient with the result that expansion takes place outside the breach. For such underexpanded sonic gas jets, v_0, ρ_0, and R_0 are the equivalent jet source properties upon expansion to ambient conditions. Underexpanded jet behavior is always apparent when the release involves pressurized volatile liquid. This section describes methods for estimating the quantities R_0, ρ_0 and v_0 at the end of the depressurization region, which serve as the initial or equivalent source conditions for the downstream atmospheric jet.

It is worth mentioning that the significant increase in the jet radius across the expansion region is due to fluid depressurization and a concomitant decrease in fluid density. Little or no entrainment of ambient air occurs in the expansion region. In contrast, the spreading of the "atmospheric pressure jet" downstream of the expansion region is due solely to entrainment of ambient air. The expansion and entrainment regions are illustrated in Fig. 1a.

2.1. Underexpanded gas jets

A brief review of the literature on models for predicting the properties of gas jets at the end of the expansion region can be found in ref. [1]. Suffice it to say that the model employed here includes both momentum and mass conservation. A momentum balance between the breach exit plane and the end of the

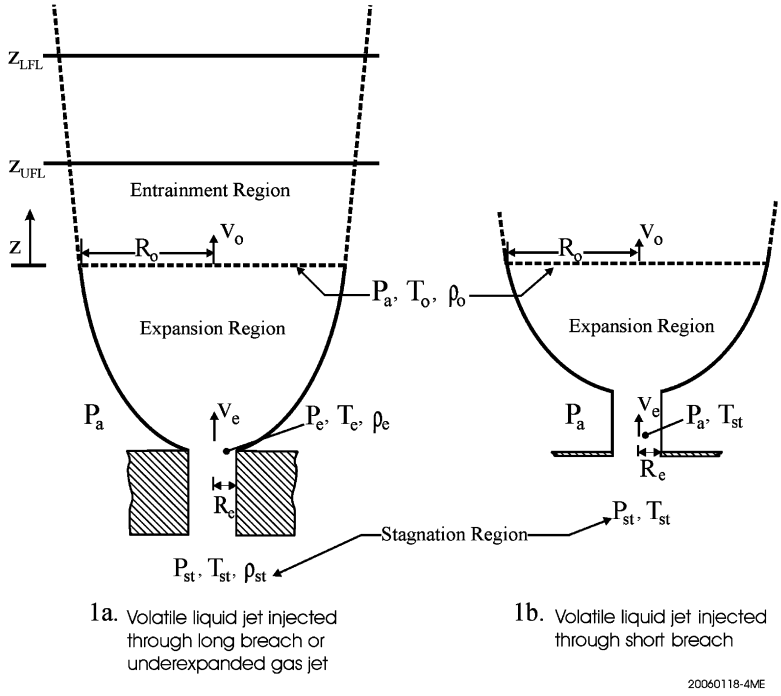

Fig. 1. Expansion zones for volatile liquid and gas jet releases. The contraction of the jet just outside the breach (vena contracta) is not shown in (b). (a) Shows the entrainment region and the top-hat model "flammability planes" downstream of the expansion region.

expansion region (see Fig. 1a) yields an expression for the equivalent source velocity v_0 of the depressurized round or plane jet:

$$v_0 = \frac{G}{\rho_e} + \frac{P_e - P_a}{G} \tag{1}$$

The effective source radius R_0 of the gas jet at the end of expansion region is obtained from the conservation of mass. For round jets

$$R_0 = R_e\left(\frac{G}{v_0\rho_0}\right)^{1/2} \quad \text{(round jets)} \tag{2}$$

while for plane jets

$$R_0 = \frac{R_e G}{v_0\rho_0} \quad \text{(plane jets)} \tag{3}$$

The quantities G, P_e and ρ_e in Eq. (1) are given by the following well-known equations for sonic gas flow through an orifice (frictional losses upstream of the exit plane are ignored):

$$G = C_D\left[\gamma P_{st}\rho_{st}\left(\frac{2}{\gamma+1}\right)^{(\gamma+1)/(\gamma-1)}\right]^{1/2} \tag{4}$$

$$P_e = P_{st}\left(\frac{2}{\gamma+1}\right)^{\gamma/(\gamma-1)}; \qquad \rho_e = \rho_{st}\left(\frac{2}{\gamma+1}\right)^{1/(\gamma-1)} \tag{5}$$

To complete the system of equations the ideal gas law is invoked to estimate the jet density ρ_0 at the end of the expansion region; that is,

$$\rho_0 = \frac{P_a}{R_{id}T_0} \tag{6}$$

In the above equation, T_0 is identified with the breach exit plane temperature

$$T_0 = T_e = T_{st}\left(\frac{2}{1+\gamma}\right) \tag{7}$$

This choice leads to an equivalent source radius R_0 that is nearly identical to that obtained with the expansion-region-mass-conservation-model of Birch et al. [6] and which resulted in a successful correlation of their natural gas jet-in-air dilution data.

2.2. Volatile liquid jets injected through a long nozzle (breach)

The volatile liquid flows through the breach from the high pressure stagnation zone to the low-pressure ambient and in so doing crosses the equilibrium pressure for the liquid temperature and disintegrates into a spray. The liquid breakup process is, in part, due to near-instantaneous liquid boiling. When the breach flow path is long, boiling takes place within the breach and a two-phase flow exists at the breach exit plane. If the breach flow path is long enough a fully developed equilibrium state exists at the breach exit plane. The available experimental data indicate that the relaxation length to equilibrium at the exit is roughly 0.1 m [7]. Just outside the breach there is a flashing (vapor evolution) and depressurizing jet expansion region (see Fig. 1a) in which the width of the jet increases rapidly and the liquid disintegrates into droplets by a flash atomization mechanism. If the breach flow path is short ($\ll$0.1 m) there is no opportunity for boiling within the breach. In this case a superheated, intact jet emerges from the breach and then suddenly boils and expands at some location downstream of the breach exit plane (see Fig. 1b). The expansion region outside the long breach is treated below. The short breach is considered in the next subsection. It is important to mention at this point that the flow within the two-phase (liquid + vapor) jet is assumed to be everywhere homogeneous.

Eqs. (1)–(3) written for pure gas jets are also valid for homogeneous two-phase jets. Thus it remains to determine G, P_e, ρ_e and ρ_0 for the volatile liquid release through a long breach. For stagnation conditions where the stagnation pressure is equal to the equilibrium pressure at the liquid temperature, the maximum discharge rate through the long breach is ($\gtrsim$0.1 m; Fauske [7]):

$$G = \frac{h_{fg}}{v_{fg}}\left(\frac{1}{T_{st}c_f}\right)^{1/2} \tag{8}$$

If the stagnation pressure is substantially larger than the equilibrium pressure corresponding to the stagnation temperature, the discharge rate through the long breach is given by the Bernoulli equation for all liquid flow:

$$G = C_D\{2\rho_f[P_{st} - P_g(T_{st})]\}^{1/2} \tag{9}$$

Note that Eqs. (8) and (9) imply equilibrium at the breach exit plane, which is a reasonable assumption for a long breach, and the pressure and density at the exit plane are set equal to the stagnation pressure and liquid density, respectively:

$$P_e = P_g(T_{st}); \qquad \rho_e = \rho_f(T_{st}) \tag{10}$$

The vapor mass fraction x_0 (quality) at the end of the expansion region is derived from an energy principle that ignores the small kinetic energy terms for a two-phase jet and equates the stagnation enthalpy with the enthalpy of the expanded and depressurized jet; namely,

$$h_{st} = h_f(P_a) + x_0 h_{fg}(P_a) \tag{11}$$

For an all-liquid release Eq. (11) becomes

$$x_0 = \frac{c_f(T_{st} - T_{bp})}{h_{fg}} \tag{12}$$

where T_{bp} is the boiling point of the liquid at ambient pressure P_a. The density ρ_0 of the fully expanded two-phase jet is related to quality x_0 by the definition

$$\rho_0 = \left[\frac{x_0}{\rho_g(P_a)} + \frac{1-x_0}{\rho_f(P_a)}\right]^{-1} \cong \frac{\rho_g(P_a)}{x_0} \tag{13}$$

2.3. Volatile liquid jets injected through a short nozzle (breach)

It can be readily shown that a momentum balance applied from the intact, superheated jet just outside the breach exit plane, where the jet pressure has been reduced to P_a, to the end of the

expansion ("explosion") region where the jet pressure returns to P_a yields

$$v_0 = v_e = \frac{G}{\rho_f} \tag{14}$$

Eqs. (2) and (3) are valid for the two-phase expansion region, where G corresponds to Bernoulli flow through the short breach that is driven by the total available pressure drop $P_{st} - P_a$; that is,

$$G = C_D[2\rho_f(P_{st} - P_a)]^{1/2} \tag{15}$$

The jet density ρ_0 at the end of the expansion region is calculated using Eqs. (12) and (13).

In closing this section we note that breaches with intermediate flow path lengths (between the limits $\ll$0.1 m and $\gtrsim$0.1 m) are difficult to deal with. While Fauske [8] has provided methods for estimating G for all two-phase flow situations, including intermediate-length breaches, no rational method is available for estimating accurately the exit plane properties P_e and ρ_e required by Eq. (1). From the point of view of predicting the total flammable mass within the downstream depressurized jet it is probably best and conservative to assume short breach ejection behavior when the flow path length is less than approximately 0.1 m, since G given by Eq. (15) for the short breach is significantly greater than G given by Eqs. (8) or (9) for the long breach. Recall from the beginning of Section 2.2 that 0.1 m is the two-phase flow relaxation length to equilibrium at the breach exit plane.

3. Flammable mass and volume in round jets

3.1. Positively buoyant fuel-gas jets directed vertically upward

In this subsection, a fuel-gas release is considered that is lighter than the outside air so that it rises in the vertical direction under the influence of both gravity and its initial momentum from the end of the expansion region where its initial (or source) conditions are

$$v = v_0, \quad Y = Y_0, \quad \rho = \rho_0, \quad R = R_0 \quad \text{at} \quad z = 0 \tag{16}$$

The quantity Y_0 in Eq. (16) is the mass fraction of fuel-gas in a release mixture composed of both fuel-gas and inert gas (taken here to be air). Very little mixing occurs between the jet and the ambient in the expansion region so that Y_0 remains constant throughout the expansion region.

The conservation equations for the top-hat (plug-flow-profile) jet model may be reduced to a single ordinary differential equation for the buoyant jet dilution factor,

$$\lambda = \frac{Y_0}{Y}, \tag{17}$$

as a function of vertical distance z. The equation is [1]

$$\frac{d\lambda}{dz} = \frac{2E_0}{R_0}\left(\frac{\rho_a}{\rho_0}\right)^{1/2}\left[\frac{1}{Fr}(\lambda^2 - 1) + 1\right]^{1/5} \tag{18}$$

where Fr is a Froude number defined by

$$Fr = \frac{8E_0 v_0^2(\rho_a/\rho_0)^{1/2}}{5gR_0(\rho_a/\rho_0 - 1)} \tag{19}$$

Once λ versus z is obtained by solving Eq. (18) the remaining jet flow properties follow from

$$\frac{v}{v_0} = \frac{1}{\lambda}\left[\frac{1}{Fr}(\lambda^2 - 1) + 1\right]^{2/5} \tag{20}$$

$$\frac{\rho}{\rho_0} = \left[\frac{\rho_0}{\rho_a} + \left(1 - \frac{\rho_0}{\rho_a}\right)\frac{1}{\lambda}\right]^{-1} \tag{21}$$

$$\frac{R}{R_0} = \left(\frac{\lambda\rho_0 v_0}{\rho v}\right)^{1/2} \tag{22}$$

Denoting z_{UFL} and z_{LFL} as the vertical distances to the top-hat model upper and lower flammability planes of the jet, respectively, the mass of flammable fuel-gas m_{flam} within the jet is (see Fig. 1a)

$$m_{flam} = \int_{z_{UFL}}^{z_{LFL}} \pi R^2 \rho Y \, dz \tag{23}$$

With the aid of Eqs. (18), (20)–(22), the above equation may be expressed solely in terms of λ. The result is

$$m_{flam} = \left(\frac{\pi R_0^3 \rho_0 Y_0}{2E_0}\right)(Fr)^{3/5}\left(\frac{\rho_0}{\rho_a}\right)^{1/2} I_{flam} \tag{24}$$

where I_{flam} is given by the integral

$$I_{flam} = \int_{\lambda_{UFL}}^{\lambda_{LFL}} \frac{\lambda \, d\lambda}{[\lambda^2 + Fr - 1]^{3/5}} \tag{25}$$

which can be integrated in closed-form to get

$$I_{flam} = \frac{5}{4}\left[\left(\frac{Y_0^2}{Y_{LFL}^2} + Fr - 1\right)^{2/5} - \left(\frac{Y_0^2}{Y_{UFL}^2} + Fr - 1\right)^{2/5}\right] \tag{26}$$

Eq. (24), together with Eq. (26), is a result reported in ref. [1]. Here we are also interested in the total flammable mass (fuel-gas + air) $m_{flam,t}$ within the jet and the volume V_{flam} of the flammable region. These quantities are defined by the integrals

$$m_{flam,t} = \int_{z_{UFL}}^{z_{LFL}} \pi R^2 \rho \, dz \tag{27}$$

and

$$V_{flam} = \int_{z_{UFL}}^{z_{LFL}} \pi R^2 \, dz \tag{28}$$

Much like with m_{flam}, by employing Eqs. (18), (20)–(22) the integrals in Eqs. (27) and (28) can be expressed in terms of λ only. After some algebra one gets

$$m_{flam,t} = \left(\frac{\pi R_0^3 \rho_0}{2E_0}\right)(Fr)^{3/5}\left(\frac{\rho_0}{\rho_a}\right)^{1/2} I_{flam,t} \tag{29}$$

$$V_{\mathrm{flam}} = \left(\frac{\pi R_0^3}{2E_0}\right)(Fr)^{3/5}\left(\frac{\rho_0}{\rho_a}\right)^{1/2} \times \left[\frac{\rho_0}{\rho_a} I_{\mathrm{flam,t}} + \left(1-\frac{\rho_0}{\rho_a}\right) I_{\mathrm{flam}}\right] \tag{30}$$

where

$$I_{\mathrm{flam,t}} = \int_{\lambda_{\mathrm{UFL}}}^{\lambda_{\mathrm{LFL}}} \frac{\lambda^2\,\mathrm{d}\lambda}{(\lambda^2+Fr-1)^{3/5}} \tag{31}$$

Unlike the integral for I_{flam} (see Eq. (25)), Eq. (31) can only be solved analytically for the singular case $Fr = 1.0$. For arbitrary Fr, Eq. (31) must be solved numerically. The possibility of representing $I_{\mathrm{flam,t}}$ by an algebraic expression has been explored. A functional form for $I_{\mathrm{flam,t}}$ is assumed that is similar to I_{flam} in Eq. (26). Specifically, an initial unknown constant coefficient A is assigned that replaces 5/4 in Eq. (26); and three initially unknown constant exponents a, b and c replace, respectively, the exponent 2 on Y_0/Y_{LFL} and on Y_0/Y_{UFL}, the exponent unity on $(Fr-1)$ and the exponent 2/5 on the groups in parenthesis in Eq. (26). The function $I_{\mathrm{flam,t}}$ is then expanded into two truncated Taylor series, one two-term series for $\lambda_{\mathrm{LFL}}^a \ll (Fr-1)^b$ and another two-term series for $\lambda_{\mathrm{UFL}}^a \gg (Fr-1)^b$. By demanding that the terms in these series equal the corresponding terms of the Taylor series expansions of the integral in Eq. (31) for $\lambda^2 \ll Fr-1$ and for $\lambda^2 \gg Fr-1$, four algebraic equations are obtained for the unknowns A, a, b and c. Solving these equations leads to the numerical values $A = 5/9$, $a = 3$, $b = 3/2$ and $c = 3/5$, thereby giving

$$I_{\mathrm{flam,t}} \cong \frac{5}{9}\left[\left(\frac{Y_0}{Y_{\mathrm{LFL}}}\right)^3 + (Fr-1)^{3/2}\right]^{3/5} - \frac{5}{9}\left[\left(\frac{Y_0}{Y_{\mathrm{UFL}}}\right)^3 + (Fr-1)^{3/2}\right]^{3/5} \tag{32}$$

The accuracy of Eq. (32) was tested by comparing it to numerically exact integrations of Eq. (31) for Froude numbers Fr ranging from 0.1 to 10^5 and for λ's ranging from 1.0 to essentially infinity. For a given Fr value the error increased from zero at $\lambda = 1.0$, reached a peak value of about 12% at some intermediate value of λ and then decreased back to zero as $\lambda \to \infty$. Note that Eq. (32) becomes nonphysical for $Fr < 1.0$. Fortunately, numerical integrations of Eq. (31) for realistic values of λ_{LFL} reveal that $I_{\mathrm{flam,t}}$ is essentially independent of Fr in the interval $0 < Fr \lesssim 1.0$. Therefore, insertion of $Fr = 1.0$ into Eq. (32) accurately represents the values of $I_{\mathrm{flam,t}}$ for all Froude numbers less than unity.

A few words of caution must be inserted here with regard to the limit of vanishing Froude number ($Fr \to 0$). In this limit of nearly pure buoyancy the jet model exploited here breaks down in the vicinity of the breach opening. The density difference between the release gas and the surrounding air, combined with the very low initial momentum of the release causes the flow to first accelerate and the flow radial boundary to contract with distance above the breach. A different model of buoyancy-driven turbulent mixing than the one used in the present jet model is required to describe mixing between the ambient air and the contracting buoyant flow (see Epstein and Burelbach [9]). An examination of Eq. (19) indicates that very low Froude numbers are only achieved in practice when the breach is rather wide (e.g., a volcanic release). Sufficiently far above the breach the low-Froude number release behaves as a plume arising from a point source of buoyancy. The closed-form asymptotic expressions for flammable fuel mass, total flammable mass and flammable volume above a point source of buoyancy are (see Eqs. (26) and (32) in the limit $Fr \to 0$; together with Eqs. (24), (29) and (30))

$$m_{\mathrm{flam}} = \frac{0.659\rho_0}{E_0^{2/5}}\left(\frac{\rho_0}{\rho_a}\right)^{1/5}\left[\frac{\dot{Q}^2 Y_0^3}{g(\rho_a/\rho_0-1)}\right]^{3/5} \times \left[\frac{1}{Y_{\mathrm{LFL}}^{4/5}} - \frac{1}{Y_{\mathrm{UFL}}^{4/5}}\right]; \quad Fr \to 0 \tag{33}$$

$$m_{\mathrm{flam,t}} = \frac{0.293\rho_0}{E_0^{2/5}}\left(\frac{\rho_0}{\rho_a}\right)^{1/5}\left[\frac{\dot{Q}^2 Y_0^3}{g(\rho_a/\rho_0-1)}\right]^{3/5} \times \left(\frac{1}{Y_{\mathrm{LFL}}^{9/5}} - \frac{1}{Y_{\mathrm{UFL}}^{9/5}}\right); \quad Fr \to 0 \tag{34}$$

$$V_{\mathrm{flam}} = \frac{0.527}{E_0^{2/5}}\left(\frac{\rho_0}{\rho_a}\right)^{1/5}\left[\frac{\dot{Q}^2 Y_0^3}{g(\rho_a/\rho_0-1)}\right]^{3/5} \times \left[\frac{5\rho_0}{9\rho_a}\left(\frac{1}{Y_{\mathrm{LFL}}^{9/5}} - \frac{1}{Y_{\mathrm{UFL}}^{9/5}}\right) + \frac{5}{4}\left(1-\frac{\rho_0}{\rho_a}\right)\left(\frac{1}{Y_0}\right) \times \left(\frac{1}{Y_{\mathrm{LFL}}^{4/5}} - \frac{1}{Y_{\mathrm{UFL}}^{4/5}}\right)\right]; \quad Fr \to 0 \tag{35}$$

where $\dot{Q} = \pi R_0^2 v_0$ is the total volumetric flow rate of the light fuel-gas mixture (fuel + air) at the point source of the buoyant jet.

Even when the release has momentum as well as positive buoyancy, the purely buoyant plume model, as represented by Eqs. (33)–(35), is valid at a sufficiently large distance z above the source. From Fig. 1 of [1] it is clear that purely buoyant plume behavior begins when $z \gtrsim 6.45(Fr\rho_0/\rho_a)^{1/2}$ for an entrainment coefficient $E_0 = 0.12$. However, to ensure that the flammable region lies within the "buoyant segment" of the release the additional criterion $Fr \lesssim 1.54\lambda_{\mathrm{UFL}}^2$ must also be obeyed.

In the limit of large Fr the asymptotic results for the flammable fuel mass, total flammable mass and the flammable volume within a pure momentum jet are obtained, namely,

$$m_{\mathrm{flam}} = \frac{\pi R_0^3 \rho_0 Y_0^3}{4E_0}\left(\frac{\rho_0}{\rho_a}\right)^{1/2}\left(\frac{1}{Y_{\mathrm{LFL}}^2} - \frac{1}{Y_{\mathrm{UFL}}^2}\right); \quad Fr \to \infty \tag{36}$$

$$m_{\mathrm{flam,t}} = \frac{\pi R_0^3 \rho_0 Y_0^3}{6E_0}\left(\frac{\rho_0}{\rho_a}\right)^{1/2}\left(\frac{1}{Y_{\mathrm{LFL}}^3}-\frac{1}{Y_{\mathrm{UFL}}^3}\right); \quad Fr\to\infty \tag{37}$$

$$V_{\mathrm{flam}} = \frac{\pi R_0^3 Y_0^3}{2E_0}\left(\frac{\rho_0}{\rho_a}\right)^{1/2}\left[\frac{\rho_0}{3\rho_a}\left(\frac{1}{Y_{\mathrm{LFL}}^3}-\frac{1}{Y_{\mathrm{UFL}}^3}\right) + \frac{1}{2}\left(1-\frac{\rho_0}{\rho_a}\right)\left(\frac{1}{Y_0}\right)\left(\frac{1}{Y_{\mathrm{LFL}}^2}-\frac{1}{Y_{\mathrm{UFL}}^2}\right)\right]; \quad Fr\to\infty \tag{38}$$

In the parentheses of Eqs. (35) and (38) the last term is generally small compared with the first term so that to good approximation for positively buoyant fuel-gas jets

$$V_{\mathrm{flam}} \cong \frac{m_{\mathrm{flam,t}}}{\rho_a} \tag{39}$$

The initial concentration of the fuel-gas in the stagnation region fuel/air mixture may be such that $Y_{\mathrm{UFL}} > Y_0 > Y_{\mathrm{LFL}}$. For this situation Y_{UFL} is replaced by Y_0 in Eqs. (26), (32)–(38).

It is worth mentioning that the theoretical jet dilution factor (or fuel mass fraction) profiles obtained from the solution of Eq. (18) is in good agreement with measurements within vertical, positively buoyant fuel-gas jets (see Fig. 1 in ref. [1]). Consequently, it is reasonable to expect Eqs. (24), (29) and (30), which are expressed as integrals of the theoretical mass fraction profiles, to give accurate estimates of m_{flam}, $m_{\mathrm{flam,t}}$ and V_{flam}.

3.2. Negatively buoyant fuel-gas jets directed vertically upward

For this case the fuel-gas mixture is heavier than air so that $\rho_0 > \rho_a$, and buoyancy is directed downward while momentum is directed upward. The conservation equations for the negative buoyancy jet are the same as those for the positive buoyancy jet except that in the former case a minus sign appears in front of Fr, which is now defined as

$$Fr = \frac{8E_0 v_0^2 (\rho_a/\rho_0)^{1/2}}{5gR_0(1-\rho_a/\rho_0)} \tag{40}$$

It turns out then that the equations presented in the previous subsection for the flammable masses and volume within a positively buoyant jet can be immediately converted to those for a negatively buoyant jet by simply modifying the integrals I_{flam} and $I_{\mathrm{flam,t}}$ (see Eqs. (25) and (31)) as follows

$$I_{\mathrm{flam}} = \int_{\lambda_{\mathrm{UFL}}}^{\lambda_{\mathrm{LFL}}} \frac{\lambda\,\mathrm{d}\lambda}{(Fr+1-\lambda^2)^{3/5}} \tag{41}$$

$$I_{\mathrm{flam,t}} = \int_{\lambda_{\mathrm{UFL}}}^{\lambda_{\mathrm{LFL}}} \frac{\lambda^2\,\mathrm{d}\lambda}{(Fr+1-\lambda^2)^{3/5}} \tag{42}$$

The first of these integrals can be evaluated in closed-form to get

$$I_{\mathrm{flam}} = \frac{5}{4}\left[\left(Fr+1-\frac{Y_0^2}{Y_{\mathrm{UFL}}^2}\right)^{2/5} - \left(Fr+1-\frac{Y_0^2}{Y_{\mathrm{LFL}}^2}\right)^{2/5}\right] \tag{43}$$

Eq. (43) does not have a physical solution if Fr falls below the critical value given by

$$Fr_{\mathrm{cr}} = \frac{Y_0^2}{Y_{\mathrm{LFL}}^2} - 1 \tag{44}$$

The upward momentum of the jet is continually decreasing with vertical distance as a result of the negative buoyancy force until it becomes zero. At this maximum height reached by the jet it spreads sideways and begins to fall back down. If $Fr < Fr_{\mathrm{cr}}$, the jet does not rise sufficiently high to be diluted below the lower flammability limit and a new model is required that is capable of following the descending jet. In practice, the gas flow at the breach is usually above 100 m s^{-1} and $Fr > Fr_{\mathrm{cr}}$ (see [1]).

Eq. (42) cannot be integrated in closed-form; it can be converted to the pair of integrals

$$I_{\mathrm{flam,t}} = \frac{1}{2}(Fr+1)^{9/10}\left[\int_0^{\lambda_{\mathrm{LFL}}^2/(Fr+1)} \frac{\xi^{1/2}\,\mathrm{d}\xi}{(1-\xi)^{3/5}} - \int_0^{\lambda_{\mathrm{UFL}}^2/(Fr+1)} \frac{\xi^{1/2}\,\mathrm{d}\xi}{(1-\xi)^{3/5}}\right] \tag{45}$$

by means of the transformation $\xi = \lambda^2/(Fr+1)$. The integrations in Eq. (45) are limited to the interval $0 \le \xi \le 1.0$ because the condition $\lambda_{\mathrm{LFL}}^2/(Fr+1) > 1.0$ is equivalent to the condition $Fr < Fr_{\mathrm{cr}}$ for jet reversal of direction before the fuel-gas is diluted below its Y_{LFL} (see Eq. (17)). The integrals in Eq. (45) are a specific form of the incomplete beta function with exponents 1/2, −3/5:

$$B(x) = \int_0^x \xi^{1/2}(1-\xi)^{-3/5}\,\mathrm{d}\xi; \quad \text{for} \quad 0 \le x \le 1.0 \tag{46}$$

A reasonably accurate algebraic representation of $B(x)$ in the interval $0 \le x \le 1.0$ may be obtained by expanding the integrand in a Taylor series about $x = 0$ and then about $x = 1.0$ and integrating term by term. The two series so obtained are complementary to one another in that they both converge rapidly in the vicinity of $x = 1/2$. Indeed only the first three terms of each series are required for good accuracy (<5% error). The series solution of Eq. (46) is then

$$B(x) = \begin{cases} \frac{2}{3}x^{3/2} + \frac{6}{25}x^{5/2} + \frac{24}{175}x^{7/2}; & 0 < x < \frac{1}{2} \\ 2.044 - \frac{5}{2}(1-x)^{2/5} + \frac{5}{14}(1-x)^{7/5}; & \frac{1}{2} < x < 1.0 \end{cases} \tag{47}$$

and the integral $I_{\mathrm{flam,t}}$ in Eq. (45) can be formally expressed as

$$I_{\mathrm{flam,t}} = \frac{1}{2}(Fr+1)^{9/10}\left[B\left(\frac{Y_0^2/Y_{\mathrm{LFL}}^2}{Fr+1}\right) - B\left(\frac{Y_0^2/Y_{\mathrm{UFL}}^2}{Fr+1}\right)\right] \tag{48}$$

Once Fr is estimated from Eq. (40) and I_{flam} and $I_{\mathrm{flam,t}}$ are estimated from Eqs. (43) and (48), the mass of flammable fuel, the total flammable mass $m_{\mathrm{flam,t}}$ and the total flammable volume V_{flam} within a negatively buoyant-round jet of fuel-gas are determined from Eqs. (24), (29) and (30). The complete expressions for m_{flam}, $m_{\mathrm{flam,t}}$ and V_{flam} for the negatively buoyant fuel-gas jet will become apparent in the next subsection.

3.3. Volatile liquid-fuel jets directed vertically upward

Volatile liquid-fuel jets are negatively buoyant jets since ρ_0 is always greater than ρ_a. Epstein and Fauske [1] demonstrated that the flammable fuel mass within a volatile liquid release is well represented by Eq. (24) with I_{flam} given by Eq. (43) for the negatively buoyant pure fuel-gas jet ($Y_0 = 1.0$), but with a numerically modified Froude number. Specifically they proposed the following equation for m_{flam} for volatile liquid-fuel releases directed vertically upward:

$$m_{\mathrm{flam}} = \left(\frac{5\pi R_0^3\rho_0}{8E_0}\right)(NFr)^{3/5}\left(\frac{\rho_0}{\rho_a}\right)^{1/2} \times \left[\left(NFr+1-\frac{1}{Y_{\mathrm{UFL}}^2}\right)^{2/5} - \left(NFr+1-\frac{1}{Y_{\mathrm{LFL}}^2}\right)^{2/5}\right] \tag{49}$$

where N is a numerical coefficient and Fr is given by Eq. (40). Eq. (49) was compared with m_{flam} predictions of an available numerical model [4] of the dispersion of volatile liquid chemicals released from pressurized storage vessels. The emitted volatile liquid-fuels considered were propylene, propane, butane, and ammonia. The numerical results were best correlated (to within 20 percent) with the choice $N = 0.62$. The reasons for the success of the "correlation", Eq. (49), which ignores two-phase jet behavior (drop evaporation and cooling), are that in the near-field-high-momentum region of the jet the shapes of the fuel and air concentration profiles depend only on jet mass, momentum and air entrainment considerations and not on energy and state equations; while far from the source, where buoyancy is important, heavier-than-air, near-isothermal single-phase gas flow prevails.

Since m_{flam} for volatile liquid-fuel jets can be represented by the m_{flam} expression for negatively buoyant fuel-gas jets it stands to reason that representations similar to Eq. (49) are valid for $m_{\mathrm{flam,t}}$ and V_{flam}. Accordingly, from Eqs. (29) and (30) with I_{flam} and $I_{\mathrm{flam,t}}$ given by Eqs. (43) and (48), respectively, it is proposed that $m_{\mathrm{flam,t}}$ and V_{flam} above a negatively-buoyant-volatile-liquid-fuel release may be calculated using

$$m_{\mathrm{flam,t}} = \left(\frac{\pi R_0^3\rho_0}{4E_0}\right)(NFr)^{3/5}(NFr+1)^{9/10}\left(\frac{\rho_0}{\rho_a}\right)^{1/2} \times \left[B\left(\frac{1/Y_{\mathrm{LFL}}^2}{NFr+1}\right) - B\left(\frac{1/Y_{\mathrm{UFL}}^2}{NFr+1}\right)\right] \tag{50}$$

$$V_{\mathrm{flam}} = \left(\frac{\pi R_0^3}{2E_0}\right)(NFr)^{3/5}\left(\frac{\rho_0}{\rho_a}\right)^{1/2} \times \left[\frac{\rho_0}{\rho_a}I_{\mathrm{flam,t}} - \left(\frac{\rho_0}{\rho_a}-1\right)I_{\mathrm{flam}}\right] \tag{51}$$

where in Eq. (51)

$$I_{\mathrm{flam}} = \frac{5}{4}\left[\left(NFr+1-\frac{1}{Y_{\mathrm{UFL}}^2}\right)^{2/5} - \left(NFr+1-\frac{1}{Y_{\mathrm{LFL}}^2}\right)^{2/5}\right] \tag{52}$$

$$I_{\mathrm{flam,t}} = \frac{1}{2}(NFr+1)^{9/10}\left[B\left(\frac{1/Y_{\mathrm{LFL}}^2}{NFr+1}\right) - B\left(\frac{1/Y_{\mathrm{UFL}}^2}{NFr+1}\right)\right] \tag{53}$$

Eqs. (49)–(53) may also be used for negatively buoyant fuel-gas jets by simply letting $N = 1.0$.

There are no published experimental data on the flammable mass or on jet dilution within vertical negatively buoyant fuel jets. However, Epstein and Fauske [1] used Eq. (18) for a negatively buoyant gas jet (with Fr replaced by $-Fr$ and defined by Eq. (40)) to derive an expression that agrees with measurements of the mass fraction at the maximum height achieved by the jet. The same approach used in ref. [1] and mentioned previously to test Eq. (49) was used to check the accuracy of Eqs. (50) and (51) for volatile liquid-fuel releases. Over 100 runs were made with the rigorous numerical dispersion model and the maximum individual difference between Eqs. (50) and (51) and the numerical results is 20%. For the sake of clarity only a selected fraction of the total number of comparisons are shown in Figs. 2 and 3. The comparisons shown in the figures were carried out for saturated ($T_{\mathrm{st}} = 27\,^{\circ}\mathrm{C}$) and subcooled [$2.0 < P_{\mathrm{st}}/P_{\mathrm{g}}\ (27\,^{\circ}\mathrm{C}) < 5.0$] liquid releases through long nozzles. The upper end values of the ranges of the exit plane radius R_e used in the calculations represented the critical values above which dilution to the LFL does not occur within an upward moving jet. These values are 8 mm for butane, 25 mm for propane, and 30 mm for propylene. In all the cases investigated for ammonia ($R_e \leq 200$ mm) dilution to the LFL occurs before the jet spreads laterally.

3.4. Fuel-gas jets and volatile liquid-fuel jets directed horizontally

The high-momentum asymptotic solution of Eq. (1), namely $\lambda = 1.0 + 2E_0(\rho_a/\rho_0)^{1/2}(z/R_0)$ for $Fr \to \infty$, was compared in ref. [1] with field measurements made downstream of large-scale-horizontal releases of liquid ammonia and hydrofluoric acid. The

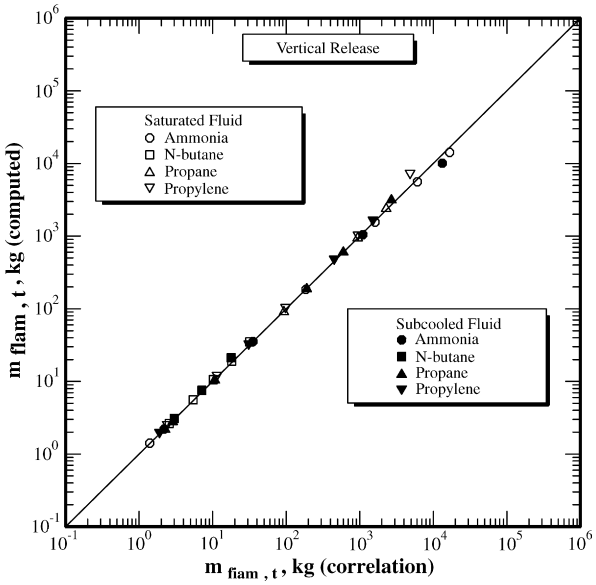

Fig. 2. Accuracy of the total flammable mass correlation, Eq. (50), for round volatile liquid-fuel jets directed vertically upwards.

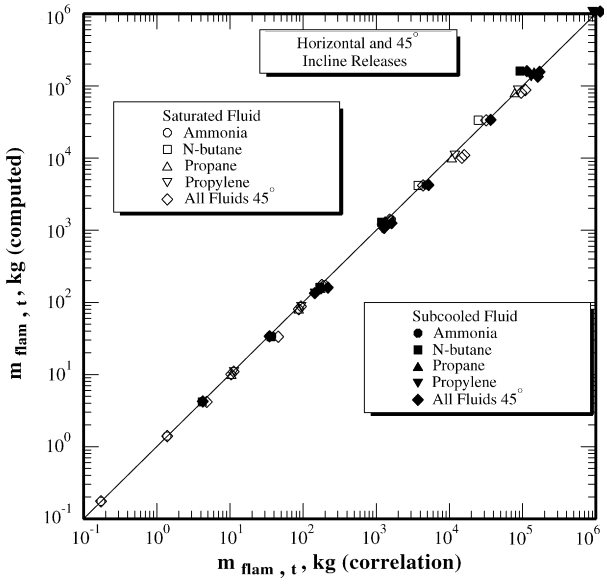

Fig. 4. Accuracy of the total flammable mass correlation, Eq. (37), for round volatile liquid-fuel jets directed horizontally or at 45° incline.

agreement of the theoretical λ with the data is within 50%. This should be regarded as encouraging considering the simplicity of the model equation and the fact that no better agreement is obtained with the much more complex dispersion model [4]. Thus it would seem that the assumption of axisymmetric, high-momentum jet flow is acceptable for the purpose of estimating m_{flam}, $m_{\text{flam,t}}$ and V_{flam} for fuel jets directed horizontally. In ref. [1] Eq. (36) for m_{flam}, with $Y_0 = 1$ for initially volatile liquid jets, was compared with the numerical dispersion model [4]; which fully accounts for elevated jet behavior (trajectory and dilution) prior to ground contact, gravity-driven lateral spreading following ground contact, and drop evaporation and turbulent entrainment of humid air. The maximum deviation between Eq. (36) for m_{flam} and the numerical dispersion model is 37% for initially ground level jets and jets initially inclined from the horizontal by as much as 45°. It follows that $m_{\text{flam,t}}$ and V_{flam} may be estimated for horizontal or moderately inclined jets by using the high-momentum asymptotes Eqs. (37) and (38) with $Y_0 = 1.0$.

The "correlations", Eqs. (37) and (38), are compared with the results of the numerical model [4] in Figs. 4 and 5 for saturated and subcooled liquid releases through long nozzles. The maximum deviation between the correlations and the numerical model of about a factor of two occurs for extremely large releases of subcooled butane. The accuracy of the correlations improve for the more volatile liquid-fuels, revealing a maximum

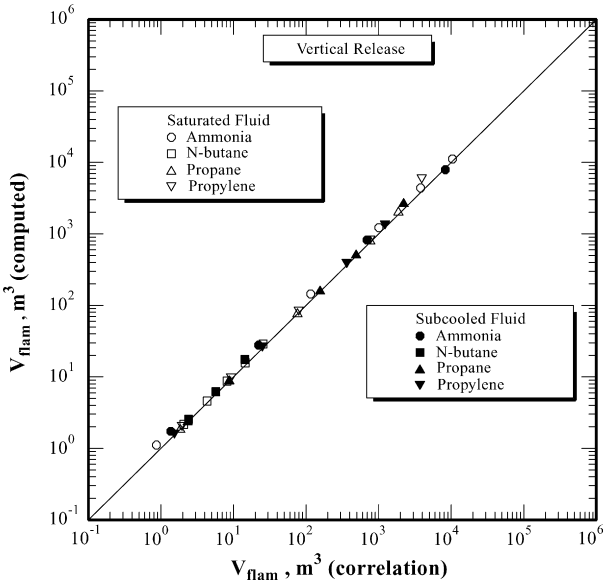

Fig. 3. Accuracy of the flammable volume correlation, Eq. (51), for round volatile liquid-fuel jets directed vertically upwards.

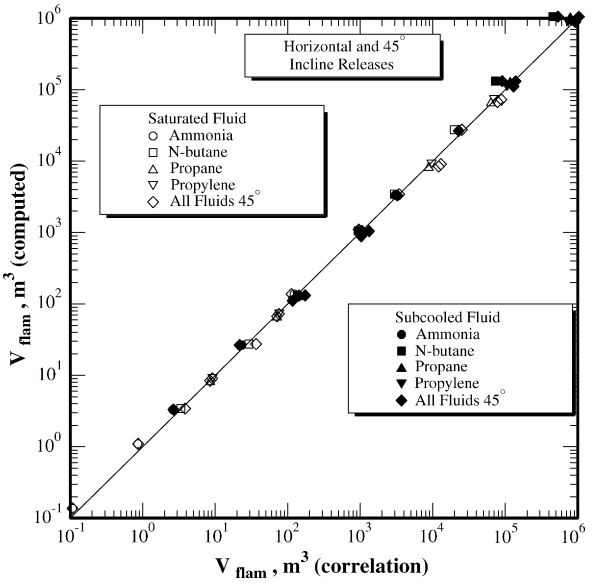

Fig. 5. Accuracy of the flammable volume correlation, Eq. (38), for round volatile liquid-fuel jets directed horizontally or at 45° incline.

individual error of about 25 percent. The correlations can be used for release angles as high as 45° without introducing errors larger than those already mentioned. Eqs. (36)–(38) can also be used for heavier-than-air fuel-gas jets directed horizontally or inclined from the horizontal by as much as 45°.

In closing this section on the round jet, it is noted that the combustion overpressure ΔP in a closed compartment is directly proportional to $m_{\mathrm{flam,t}}$ (see Eq. (82)). Thus, for example, if the maximum departure of Eq. (32) from the numerical dispersion model predictions of $m_{\mathrm{flam,t}}$ is 25%, the corresponding percentage departure in calculating ΔP is also 25%. A departure of 25% for m_{flam} is probably insignificant in evaluating blast wave effects from semi-confined vapor cloud explosions since uncertainties associated with blast-wave model parameters such as the flame speed are considerably larger than 25%.

4. Flammable mass and volume in plane jets

4.1. Positively buoyant fuel-gas jets directed vertically upward

The initial (or source) conditions for the buoyant plane jet ($\rho_a > \rho_0$) are the same as those for the round jet and are given in Eq. (16). Now R_0 and R refer to the half-width of the plane jet at the source and downstream of the source, respectively. Much like the round jet, the conservation equations for the isothermal plane jet top-hat model may be reduced to a single ordinary differential equation for the jet dilution factor λ as a function of vertical distance z:

$$\frac{\mathrm{d}\lambda}{\mathrm{d}z} = \frac{E_0\rho_a}{R_0\rho_0\lambda}\left[\frac{1}{Fr}(\lambda^3 - 1) + 1\right]^{1/3} \tag{54}$$

where

$$Fr = \frac{E_0 v_0^2}{gR_0(1 - \rho_0/\rho_a)} \tag{55}$$

It is important to mention that in the plane jet model, upon which Eq. (54) is based, the velocity of air entrainment at the jet boundary is assumed to equal $E_0 v$, whereas in the round jet model the air entrainment velocity is given by $E_0(\rho/\rho_a)^{1/2}v$. These entrainment law functions are requirements for similarity solutions of the plane and round jet conservation equations, respectively [Delichatsios, 10]. The entrainment velocity function for round jets is known to be correct from the laboratory work of Ricou and Spalding [11]. The entrainment velocity function for the plane jet with large density variations still awaits experimental confirmation.

The velocity v, density ρ and half-width R as functions of λ alone are as follows:

$$\frac{v}{v_0} = \frac{1}{\lambda}\left[\frac{1}{Fr}(\lambda^3 - 1) + 1\right]^{1/3} \tag{56}$$

$$\frac{\rho}{\rho_0} = \left[\frac{\rho_0}{\rho_a} + \left(1 - \frac{\rho_0}{\rho_a}\right)\frac{1}{\lambda}\right]^{-1} \tag{57}$$

$$\frac{R}{R_0} = \frac{\lambda\rho_0 v_0}{\rho v} \tag{58}$$

The mass of flammable fuel-gas, the total flammable mass (fuel + air) and the volume of the flammable region within the jet are by definition

$$m_{\mathrm{flam}} = 2L\int_{z_{\mathrm{UFL}}}^{z_{\mathrm{LFL}}} R\rho Y\,\mathrm{d}z \tag{59}$$

$$m_{\mathrm{flam,t}} = 2L\int_{z_{\mathrm{UFL}}}^{z_{\mathrm{LFL}}} R\rho\,\mathrm{d}z \tag{60}$$

$$V_{\mathrm{flam}} = 2L\int_{z_{\mathrm{UFL}}}^{z_{\mathrm{LFL}}} R\,\mathrm{d}z \tag{61}$$

In the above equations L is the lateral dimension of the plane jet.

Combining Eqs. (54)–(61) yields the following exact solution for m_{flam} and approximate expressions for $m_{\mathrm{flam,t}}$, and V_{flam}

$$m_{\mathrm{flam}} = \frac{2LR_0^2Y_0\rho_0^2Fr^{2/3}}{E_0\rho_a}I_{\mathrm{flam}} \tag{62}$$

$$m_{\mathrm{flam,t}} = \frac{2LR_0^2\rho_0^2Fr^{2/3}}{E_0\rho_a}I_{\mathrm{flam,t}} \tag{63}$$

$$V_{\mathrm{flam}} = \frac{2LR_0^2\rho_0Fr^{2/3}}{E_0\rho_a}\left[\frac{\rho_0}{\rho_a}I_{\mathrm{flam,t}} + \left(1 - \frac{\rho_0}{\rho_a}\right)I_{\mathrm{flam}}\right] \tag{64}$$

where

$$I_{\mathrm{flam}} = \int_{\lambda_{\mathrm{UFL}}}^{\lambda_{\mathrm{LFL}}} \frac{\lambda^2\,\mathrm{d}\lambda}{(\lambda^3 + Fr - 1)^{2/3}} = \left(\frac{Y_0^3}{Y_{\mathrm{LFL}}^3} + Fr - 1\right)^{1/3} - \left(\frac{Y_0^3}{Y_{\mathrm{UFL}}^3} + Fr - 1\right)^{1/3} \tag{65}$$

$$I_{\mathrm{flam,t}} = \int_{\lambda_{\mathrm{UFL}}}^{\lambda_{\mathrm{LFL}}} \frac{\lambda^3\,\mathrm{d}\lambda}{(\lambda^3 + Fr - 1)^{2/3}} = \frac{1}{2}\left(\frac{Y_0^4}{Y_{\mathrm{LFL}}^4} + (Fr - 1)^{4/3}\right)^{1/2} - \frac{1}{2}\left(\frac{Y_0^4}{Y_{\mathrm{UFL}}^4} + (Fr - 1)^{4/3}\right)^{1/2} \tag{66}$$

The right-hand side of Eq. (66) approximates the exact numerical integrations of $I_{\mathrm{flam,t}}$ to within 12% (see discussion above and below Eq. (32)).

For a plane plume emanating from a line source of pure buoyancy ($Fr \to 0$) Eqs. (62)–(66) simplify to

$$m_{\mathrm{flam}} = \frac{0.794LY_0^2\rho_0^2}{E_0^{1/3}\rho_a}\left[\frac{\dot{Q}^2}{g(1 - \rho_0/\rho_a)L^2}\right]^{2/3} \times \left(\frac{1}{Y_{\mathrm{LFL}}} - \frac{1}{Y_{\mathrm{UFL}}}\right); \quad Fr \to 0 \tag{67}$$

$$m_{\mathrm{flam,t}} = \frac{0.397 L Y_0^2 \rho_0^2}{E_0^{1/3}\rho_a}\left[\frac{\dot{Q}^2}{g(1-\rho_0/\rho_a)L^2}\right]^{2/3} \times \left(\frac{1}{Y_{\mathrm{LFL}}^2} - \frac{1}{Y_{\mathrm{UFL}}^2}\right); \quad Fr \to 0 \tag{68}$$

$$V_{\mathrm{flam}} = \frac{0.794 L Y_0^2 \rho_0}{E_0^{1/3}\rho_a}\left[\frac{\dot{Q}^2}{g(1-\rho_0/\rho_a)L^2}\right]^{2/3} \times \left[\frac{1}{2}\frac{\rho_0}{\rho_a}\left(\frac{1}{Y_{\mathrm{LFL}}^2} - \frac{1}{Y_{\mathrm{UFL}}^2}\right) + \left(1-\frac{\rho_0}{\rho_a}\right)\left(\frac{1}{Y_0}\right)\left(\frac{1}{Y_{\mathrm{LFL}}} - \frac{1}{Y_{\mathrm{UFL}}}\right)\right]; \quad Fr \to 0 \tag{69}$$

where $\dot{Q} = 2R_0 L v_0$ is the total volumetric flow rate of the purely buoyant gas mixture (fuel + air) at the line source.

For high-momentum plane jets ($Fr \to \infty$), Eqs. (62)–(66) become

$$m_{\mathrm{flam}} = \frac{2LR_0^2 Y_0^4 \rho_0^2}{3E_0\rho_a}\left(\frac{1}{Y_{\mathrm{LFL}}^3} - \frac{1}{Y_{\mathrm{UFL}}^3}\right); \quad Fr \to \infty \tag{70}$$

$$m_{\mathrm{flam,t}} = \frac{LR_0^2 Y_0^4 \rho_0^2}{2E_0\rho_a}\left(\frac{1}{Y_{\mathrm{LFL}}^4} - \frac{1}{Y_{\mathrm{UFL}}^4}\right); \quad Fr \to \infty \tag{71}$$

$$V_{\mathrm{flam}} = \frac{2LR_0^2 Y_0^4 \rho_0}{E_0\rho_a}\left[\frac{\rho_0}{4\rho_a}\left(\frac{1}{Y_{\mathrm{LFL}}^4} - \frac{1}{Y_{\mathrm{UFL}}^4}\right) + \frac{1}{3}\left(1-\frac{\rho_0}{\rho_a}\right)\left(\frac{1}{Y_0}\right)\left(\frac{1}{Y_{\mathrm{LFL}}^3} - \frac{1}{Y_{\mathrm{UFL}}^3}\right)\right]; \quad Fr \to \infty \tag{72}$$

4.2. Negatively buoyant fuel-gas jets directed vertically upward

The appropriate Froude number for the negatively buoyant plane jet is

$$Fr = \frac{E_0 v_0^2}{gR_0(\rho_0/\rho_a - 1)} \tag{73}$$

Following essentially the same mathematical steps taken for the round jet, the integrals I_{flam} and $I_{\mathrm{flam,t}}$ for the negatively buoyant plane jet are

$$I_{\mathrm{flam}} = \int_{\lambda_{\mathrm{UFL}}}^{\lambda_{\mathrm{LFL}}} \frac{\lambda^2\,\mathrm{d}\lambda}{(Fr+1-\lambda^3)^{2/3}} = \left(Fr+1-\frac{Y_0^3}{Y_{\mathrm{UFL}}^3}\right)^{1/3} - \left(Fr+1-\frac{Y_0^3}{Y_{\mathrm{LFL}}^3}\right)^{1/3} \tag{74}$$

$$I_{\mathrm{flam,t}} = \int_{\lambda_{\mathrm{UFL}}}^{\lambda_{\mathrm{LFL}}} \frac{\lambda^3\,\mathrm{d}\lambda}{(Fr+1-\lambda^3)^{2/3}} = \frac{1}{3}(Fr+1)^{2/3}\left[B\left(\frac{Y_0^3/Y_{\mathrm{LFL}}^3}{Fr+1}\right) - B\left(\frac{Y_0^3/Y_{\mathrm{UFL}}^3}{Fr+1}\right)\right] \tag{75}$$

where $B(x)$ in Eq. (75) is the incomplete beta function

$$B(x) = \int_0^x \xi^{1/3}(1-\xi)^{-2/3}\,\mathrm{d}\xi \tag{76}$$

The Taylor series approximation of $B(x)$ in Eq. (76) is

$$B(x) = \begin{cases} \frac{3}{4}x^{4/3} + \frac{2}{7}x^{7/3} + \frac{1}{6}x^{10/3}; & 0 < x < \frac{1}{2} \\ 2.65 - 3(1-x)^{1/3} + \frac{1}{4}(1-x)^{4/3}; & \frac{1}{2} < x < 1.0 \end{cases} \tag{77}$$

Once Fr, I_{flam} and $I_{\mathrm{flam,t}}$ are calculated from Eqs. (73)–(75), the flammable fuel mass m_{flam}, the total flammable mass $m_{\mathrm{flam,t}}$ and the flammable volume V_{flam} within a negatively buoyant plane jet are estimated from Eqs. (62), (63) and (64), respectively.

Note from Eqs. (74) and (75) that I_{flam} and $I_{\mathrm{flam,t}}$ are nonphysical if Fr falls below $\mathrm{Fr_{cr}} = Y_0^3/Y_{\mathrm{LFL}}^3 - 1$. A similar criterion was already discussed for the round jet (see Eq. (44)). If $Fr < Fr_{\mathrm{cr}}$ the plane jet is not diluted below the fuel-gas Y_{LFL} before the jet velocity is reduced to zero and the jet begins to spread out laterally and descend. Consider the subsonic release of pure propane ($Y_0 = 1.0$, $\rho_0 = 1.79\,\mathrm{kg\,m^{-3}}$, $Y_{\mathrm{LFL}} = 0.032$) into ambient air ($\rho_a = 1.18\,\mathrm{kg\,m^{-3}}$). The entrainment coefficient for the plane jet is $E_0 = 0.08$. This value was inferred here from available plane-jet spreading rate data (Bashir and Uberoi [12]). A physical propane release (viz. $Fr > Fr_{\mathrm{cr}}$) requires that $R_0 < 5.17 \times 10^{-7}\, v_0^2$, where R_0 and v_0 are in units of m and $\mathrm{m\,s^{-1}}$. If the propane gas flow at the orifice (slot opening) is nearly sonic, $v_0 = 256\,\mathrm{m\,s^{-1}}$ and physical solutions are obtained for slot widths $R_0 < 3.39 \times 10^{-2}$ m. At $v_0 = 25\,\mathrm{m\,s^{-1}}$ the permissible slot widths are less than $R_0 = 3.23 \times 10^{-4}$ m. Such small slot widths are of practical interest, mainly for assessing fuel-gas leaks emanating from fine cracks in pipes or vessel walls. The treatment of large slot widths requires a more elaborate model that is capable of following the descending portion of the jet flow field.

4.3. Volatile liquid-fuel jets directed vertically upward

The jet reversal difficulty, mentioned in the foregoing for negatively buoyant fuel-gas jets, imposes an even greater limitation upon the plane-upward-directed volatile-fuel jet-model in that for many liquid-fuel materials the model is rendered invalid for slit-widths larger than a few tens of microns. Nevertheless, for the sake of completeness, the model equations are briefly discussed in this subsection.

Much like what was done for round jets, the solution to this problem is taken to be the same as that derived above for negatively buoyant fuel-gas jets directed vertically upward; namely, Eqs. (62)–(64) together with Eqs. (73)–(75), but with

$Y_0 = 1.0$ and Fr replaced by NFr. The validity of the modified Froude number approach to the prediction of flammable masses and volumes within volatile, negatively-buoyant plane jets was examined by comparing the predictions obtained using Eqs. (62)–(64) and (73)–(75) with those of a numerical solution of the complete set of conservation equations for the plane jet. Space limitations preclude a detailed description of the numerical model. Suffice it to say that the model is a homogeneous equilibrium model that fully accounts for the effects of liquid phase evaporative cooling in the near field of the jet. Recall that the functional forms represented by Eqs. (62)–(64), (74) and (75) are based on isothermal jet flow. Reasonable agreement between these equations and the numerical model was obtained with the same Froude number numerical correction factor $N = 0.62$ used for round jets. Of course the comparisons were only carried out for those fuel releases that obeyed the criterion $NFr > 1/Y_{\mathrm{LFL}}^3 - 1$ required for jet dilution to the Y_{LFL} before jet reversal. For saturated liquid butane released at 300 K this criterion translates to $R_e \leq 19.5$ μm. For a saturated liquid ammonia release at 300 K valid solutions demand $R_e \leq 2.45$ mm. Thus the present model of a plane volatile fuel jet released vertically is not suitable for a broad range of applications.

4.4. Fuel-gas jets and volatile liquid-fuel jets directed horizontally

The previously mentioned experience with round jets suggests that m_{flam}, $m_{\mathrm{flam,t}}$ and V_{flam} may be accurately and readily estimated for horizontal, heavier-than-air-plane jets by ignoring the effects of buoyancy over the distance that the jet is flammable and using the high-momentum ($Fr \to \infty$) asymptotic forms given by Eqs. (70)–(72). For horizontal volatile liquid releases $Y_0 = 1.0$ in these equations.

5. Fuel concentration in flammable region of release

An indicator of the potential explosiveness of the fuel/air cloud produced by a plume or jet release is the average composition of the flammable region and how close it is to the stoichiometric proportion. The average fuel mass fraction $\bar{Y}$ in the flammable region above a round point source of fuel-gas buoyancy is (see Eqs. (33) and (34)).

$$\bar{Y} = \frac{m_{\mathrm{flam}}}{m_{\mathrm{flam,t}}} = \frac{9}{4}\left(\frac{1/Y_{\mathrm{LFL}}^{4/5} - 1/Y_{\mathrm{UFL}}^{4/5}}{1/Y_{\mathrm{LFL}}^{9/5} - 1/Y_{\mathrm{UFL}}^{9/5}}\right); \quad Fr \to 0 \tag{78}$$

For a round, high-momentum jet of fuel-gas or volatile liquid-fuel (see Eqs. (36) and (37))

$$\bar{Y} = \frac{3}{2}\left(\frac{1/Y_{\mathrm{LFL}}^2 - 1/Y_{\mathrm{UFL}}^2}{1/Y_{\mathrm{LFL}}^3 - 1/Y_{\mathrm{UFL}}^3}\right); \quad Fr \to \infty \tag{79}$$

For plane, purely buoyant plumes of fuel-gas, Eqs. (67) and (68) yield

$$\bar{Y} = 2.0\left(\frac{1/Y_{\mathrm{LFL}} - 1/Y_{\mathrm{UFL}}}{1/Y_{\mathrm{LFL}}^2 - 1/Y_{\mathrm{UFL}}^2}\right); \quad Fr \to 0 \tag{80}$$

Table 1
$\bar{Y}/Y_{\mathrm{stoic}}$ for purely buoyant gas releases

Fuel	Y_{stoic}	$\bar{Y}/Y_{\mathrm{stoic}}$	
		Point source	Line source
Hydrogen	0.0281 (0.295)	0.221 (0.281)	0.201 (0.257)
Ammonia	0.141 (0.218)	0.892 (0.901)	0.886 (0.895)
Methane	0.0548 (0.0948)	0.80 (0.806)	0.784 (0.791)

Values or ratios of values in parentheses are in volume percent

and for plane, high-momentum jets of fuel-gas or volatile liquid-fuel (see Eqs. (70) and (71))

$$\bar{Y} = \frac{4}{3}\left(\frac{1/Y_{\mathrm{LFL}}^3 - 1/Y_{\mathrm{UFL}}^3}{1/Y_{\mathrm{LFL}}^4 - 1/Y_{\mathrm{UFL}}^4}\right); \quad Fr \to \infty \tag{81}$$

The average fuel mass fraction divided by the stoichiometric fuel mass fraction ($\bar{Y}/Y_{\mathrm{stoic}}$) for purely buoyant fuel-gas releases and for high-momentum fuel-gas and volatile liquid-fuel releases are listed for several fuel materials in Tables 1 and 2, respectively. The average hydrogen concentration is well below its stoichiometric concentration. In fact its average concentration of 5.8 volume percent in a round-high-momentum jet is in the range 4–8% where combustion of hydrogen-air mixtures is incomplete (Ratzel [13]). Indeed, the average hydrogen concentration in buoyant plumes and momentum jets is so low (<8.3 vol.%) that one may judge their flammable regions to be not detonable. The detonability range is 13–70 vol.% hydrogen at 300 K (Berman [14] and Atkinson et al. [15]). The average compositions of the other fuels listed in Tables 1 and 2 vary from about one-half to nearly the stoichiometric proportion. Thus whether or not a jet or plume will produce the maximum possible pressure upon igniting depends very much on the fuel material that is released.

It is worth mentioning that Sadee et al. [16] as part of their assessment of the Flixborough plant accident, estimated that a round jet release of cyclohexane contains about a 1.85% by volume flammable fuel/air mixture. Their estimate was obtained by integrating the concentration profiles in the Gaussian model of the jet; it agrees very well with the present top-hat-model estimate of $2.27 \times 0.84 = 1.92\%$ fuel by volume (see Table 2).

So far in this section attention has focused on $\bar{Y}$ within pure buoyant plumes or pure momentum jets. The expression for

Table 2
$\bar{Y}/Y_{\mathrm{stoic}}$ for high-momentum fuel-gas or volatile-liquid-fuel releases

Fuel	Y_{stoic}	$\bar{Y}/Y_{\mathrm{stoic}}$	
		Round jets	Plane jets
Hydrogen	0.0281 (0.295)	0.153 (0.199)	0.136 (0.178)
Ammonia	0.141 (0.218)	0.855 (0.866)	0.828 (0.841)
Methane	0.0548 (0.0948)	0.720 (0.728)	0.674 (0.683)
Butane	0.0607 (0.0312)	0.841 (0.837)	0.772 (0.767)
Propylene	0.0634 (0.0445)	0.784 (0.780)	0.719 (0.715)
Cyclohexane	0.0632 (0.0227)	0.850 (0.844)	0.773 (0.766)
Ethylene	0.0634 (0.0653)	0.616 (0.617)	0.550 (0.551)
Propane	0.06 (0.0402)	0.759 (0.755)	0.697 (0.693)

Values or ratios of values in parentheses are in volume percent.

the average fuel mass fraction $\bar{Y}$ in the flammable region of a positively-buoyant-round jet (with release momentum) of initially pure fuel ($Y_0 = 1.0$) directed vertically upward may be easily constructed from Eqs. (24), (26), (29) and (32). The expression, which is omitted here for the sake of brevity, shows that $\bar{Y}$ decreases monotonically with Fr as Fr is increased from $Fr = 0$ for purely buoyant jets to $Fr \to \infty$ for high-momentum jets. The magnitude of the decrease in $\bar{Y}$ is readily obtained from Tables 1 and 2. For example $\bar{Y}$ decreases from 6.21×10^{-3} (see Table 1) in a purely-buoyant-round-release of hydrogen to 4.3×10^{-3} in a high-momentum round jet of hydrogen (see Table 2). The corresponding decrease in $\bar{Y}$ is smaller for ammonia releases, from 0.126 to 0.121. Positively buoyant plane jets exhibit the same $\bar{Y}$ versus Fr trend as positively buoyant round jets.

The equations for $\bar{Y}$ within negatively-buoyant-round-fuel-gas jets (for $Y_0 = 1.0$) and within negatively-buoyant-round-volatile liquid-fuel jets are readily derived from Eqs. (49) and (50), where $N = 1.0$ for fuel-gas jets and $N = 0.62$ for volatile liquid-fuels. The equations show that $\bar{Y}$ increases monotonically with Fr as Fr is increased from its minimum physical value $Fr_{cr} = (1/Y_{LFL}^2 - 1)/N$, corresponding to simultaneous jet dilution to the LFL and zero upward jet velocity, to the high-momentum limit $Fr \to \infty$. For all the fuel materials considered here $\bar{Y}$ at $Fr = Fr_{cr}$ is about 82% of $\bar{Y}$ at $Fr = \infty$ (for round jets). For negatively buoyant plane jets $\bar{Y}$ at $Fr = Fr_{cr}$ is about 85% of $\bar{Y}$ at $Fr = \infty$.

6. Combustion overpressure calculations

The combustion of fuel jets/plumes released to the outside atmosphere generates insignificant overpressure (Seifert and Giesbrecht [17]). Wiekema [18] analyzed numerous vapor cloud explosion accidents and concluded that all of these incidents occurred in semi-confined situations where buildings or other large structures are "submerged" in the cloud. Apparently flame acceleration between structures up to and beyond the speed required to generate destructive overpressure ($\sim$100 m s^{-1}) occurred during these incidents. Assessment of blast wave effects from semi-confined vapor cloud explosions is a difficult business because the severity of the blast depends not only on the mass of fuel available to burn but also on the magnitude of the flame speed, which varies dramatically depending on the volume fraction of the vapor cloud occupied by structure. Blast pressure predictions (van den Berg [19]; Tang and Baker [20]) are based on a family of so-called blast curves in which the overpressure is plotted versus distance scaled by the cubed root of the chemical energy stored in the vapor cloud. The chemical energy is simply the product of the heat of combustion of the fuel and the mass m_{flam} of the fuel in the flammable region of the cloud. The quantity m_{flam} is easily determined by using the expressions derived in Epstein and Fauske [1] and repeated here. Unfortunately the appropriate blast curve to use for a specific case of vapor cloud partial confinement requires an empirical determination of the initial strength of the blast (van den Berg [19]) or of the flame speed (Tang and Baker [20]).

The application of the equations presented here for m_{flam} and $m_{flam,t}$ are perhaps best illustrated by considering the case of complete confinement. Accidental fuel releases into closed-compartment atmospheres followed by deflagrations produce spatially uniform overpressures, the magnitude of which depend mainly on the ratio of the flammable fuel/air mixture mass to that of the compartment air. The combustion pressure rise ΔP in the room can be predicted with the Lewis and von Elbe [21] formula

$$\Delta P = (P_{max} - P_a)\frac{m_{flam,t}}{m_a} \tag{82}$$

where m_a is the mass of the flammable fuel/air mixture of average fuel concentration $\bar{Y}$, as predicted for the plume or jet release, assuming that the mixture fills the entire room (approximated here as the total mass of air in the room prior to the release) and P_{max} is the absolute combustion pressure that would be achieved if the flammable mixture fills the entire room.

The ratio of peak pressure P_{max} to initial room pressure P_a can be estimated from the ideal gas law

$$\frac{P_{max}}{P_a} = \frac{T_{max}}{T_a} \tag{83}$$

where the justifiable assumption has been made that the molecular weight of the unburned fuel/air mixture is equal to the molecular weight of the combustion products. In Eq. (83) the temperature T_{max} corresponds to the adiabatic flame temperature of the fuel-air mixture. Thermochemical equilibrium calculations of adiabatic flame temperatures T_{max} versus $\bar{Y}$ are tabulated or presented graphically in several textbooks or handbooks (see, e.g., Strehlow [22]).

Example. A 0.45-kg cylinder of liquid propane is stored in a 50.0-m^3 room of air at $T_a = 27\,^\circ$C (300 K). It is desired to determine the combustion overpressure in the room following an accidental release of the propane due to the failure of the cylinder's short and round, 1.0-mm diameter orifice ($R_e = 0.5$ mm, $C_D = 0.61$). Two cases are of interest: an upright cylinder resulting in a negatively buoyant jet, and a cylinder lying on its side resulting in a pure momentum jet. The pertinent thermophysical properties of the saturated propane are $P_g(T_a) = 10^6$ Pa, $\rho_f = 582$ kg m^{-3}, $c_f = 2680$ J kg^{-1} K^{-1}, $\rho_g(P_a) = 2.42$ kg m^{-3}, $Y_{LFL} = 0.0316$, $Y_{UFL} = 0.1378$, $T_{bp} = 231$ K, $h_{fg} = 3.31 \times 10^5$ J kg^{-1}.

Solution: Suppose at first that the entire cylinder's inventory of propane completely mixes uniformly with the room air. A 50-m^3 room of air at 27 °C (density $\rho_a = 1.19$ kg m^{-3}) contains $m_a = 59.5$ kg of air. Therefore, the mass fraction of 0.45 kg of propane mixed with the room air is 7.56×10^{-3}. This concentration is only 24% of the propane lower flammability limit. In this example, then, turbulent mixing of the propane jet with the room air dictates the mass of propane that is available for combustion.

Since the liquid propane is stored at room temperature, in Eq. (12) $T_{st} = T_a$ and $x_0 = 0.559$ and $\rho_0 = 4.32$ kg m^{-3} (see Eq. (13)). From Eqs. (14) and (15) for a short orifice $v_0 = 33.9$ m s^{-1} and $G = 1.97 \times 10^4$ kg m^{-2} s^{-1}, and from Eq. (2) the radius of the depressurized two-phase jet is $R_0 = 5.81 \times 10^{-3}$ m. The Froude

number for the vertical propane jet is $Fr = 2.34 \times 10^3$ (see Eq. (40)). Inserting these estimates into Eqs. (49) and (50) for the negatively buoyant propane jet gives

$$m_{\text{flam}} = 1.65 \times 10^{-2}\,\text{kg}, \quad m_{\text{flam,t}} = 0.38\,\text{kg},$$
$$\bar{Y} = \frac{m_{\text{flam}}}{m_{\text{flam,t}}} = 4.34 \times 10^{-2} \tag{84}$$

The adiabatic flame temperature of a propane/air mixture of mass fraction 4.34×10^{-2} (2.9×10^{-2} vol.%) is $T_{\max} = 1900\,\text{K}$ [22] and the maximum explosion pressure for a room completely filled with the propane/air mixture is, from Eq. (83), $P_{\max} = 6.33$ atm. Finally, from Eq. (82), the combustion pressure rise is

$$\Delta P = 0.034\,\text{atm (for vertical propane cylinder)} \tag{85}$$

The propane jet issuing from the horizontal propane cylinder behaves as a pure momentum jet and the appropriate equations for m_{flam} and $m_{\text{flam,t}}$ are Eqs. (36) and (37), which yield

$$m_{\text{flam}} = 1.12 \times 10^{-2}\,\text{kg}, \quad m_{\text{flam,t}} = 0.264\,\text{kg},$$
$$\bar{Y} = \frac{m_{\text{flam}}}{m_{\text{flam,t}}} = 4.54 \times 10^{-2} \tag{86}$$

From the graphs in ref. [22], $T_{\max} = 1960\,\text{K}$ and $P_{\max} = 6.53$ atm (see Eq. (83)). Substituting these results into Eq. (82) gives

$$\Delta P = 0.025\,\text{atm (for horizontal propane cylinder)} \tag{87}$$

A comparison of Eq. (85) with Eq. (87) reveals that ignition of the propane/air jet emanating from the vertical propane cylinder results in a room pressure rise ΔP that is about 36% higher than the ΔP following ignition of the sideways propane jet.

It can be shown from Eqs. (37) and (50) that, for fixed stagnation conditions, $m_{\text{flam},t}$ for a negatively buoyant jet is always larger than $m_{\text{flam,t}}$ for a pure momentum jet, by as much as a factor of three for round jets.

7. Conclusions

Simply analytical expressions have been developed to predict the flammable fuel mass, the total flammable mass (fuel + entrained air) and the volume of the flammable region within a buoyant fuel-jet release. These expressions which focus on a minimum number of basic dimensionless parameters incorporate both gaseous and volatile liquid-fuel releases and include the effects of release momentum, release buoyancy (positive or negative) and release orifice geometry (slot or round). A useful byproduct of these expressions are simple functional relationships between the average fuel mass concentration in the flammable zone of the release and the upper and lower flammability mass concentrations of the fuel. The relationships for the average fuel mass fraction clearly indicate that, for a fixed release mass, the combustion overpressure following ignition of a hydrogen/air release cloud is significantly lower than that due to ignition of a hydrocarbon/air release cloud. A numerical example involving a liquid propane release showed that the mass of the flammable region within a negatively buoyant jet is greater than that in a high momentum jet. In this connection, a method for dealing with lateral spreading and the descent of the flammable region in large, negatively buoyant jets would constitute a useful next step, especially for plane-volatile-liquid jets.

References

[1] M. Epstein, H.K. Fauske, Mass of flammable material produced by continuous fuel-gas and volatile liquid-fuel releases, Combust. Sci. Technol. 171 (2001) 89–118.
[2] J.G. Marshall, The size of flammable clouds arising from continuous releases into the atmosphere, I. Chem. E. Symp. Ser. No. 49 (1977) 99–109.
[3] V.D. Long, Estimation of the extent of hazard areas around a vent, in: 2nd Symposium on Chemical Process Hazards (Inst. Chem. Eng.), 1963, pp. 6–14.
[4] M. Epstein, H.K. Fauske, G.M. Hauser, A model of the dilution of a forced two-phase chemical plume in a horizontal wind, J. Loss Prev. Process Ind. 3 (1990) 280–290.
[5] M. Epstein, H.K. Fauske, Flammable mass and length of a variable-density buoyant fuel jet: Gaussian versus top-hat profiles, Combust. Sci. Technol. 175 (2003) 1333–1346.
[6] A.D. Birch, D.R. Brown, M.G. Dodson, F. Swaffield, The structure and concentration decay of high pressure jets of natural gas, Combust. Sci. Technol. 36 (1984) 249–261.
[7] H.K. Fauske, Flashing flows: some practical guidelines for emergency releases, Plant/Oper. Progress 4 (1985) 132–134.
[8] H.K. Fauske, Determine two-phase flows during releases, Chem. Eng. Progress (1999) 55–58.
[9] M. Epstein, J.P. Burelbach, Vertical mixing above a steady circular source of buoyancy, Int. J. Heat Mass Transfer 44 (2001) 525–536.
[10] M.A. Delichatsios, On the similarity of velocity and temperature profiles in strong (variable density) turbulent buoyant plumes, Combust. Sci. Technol. 60 (1988) 253–266.
[11] F.B. Ricou, D.B. Spalding, Measurements of entrainment of axisymmetrical turbulent jets, J. Fluid Mech. 11 (1961) 21–32.
[12] J. Bashir, M.S. Uberoi, Experiments on turbulent structure and heat transfer in a two-dimensional jet, Phys. Fluids 18 (1975) 405–410.
[13] A.C. Ratzel, Data Analysis for Nevada Test Site (NTS) Premixed Combustion Tests, NUREG/CR-4138 SAND85-0135, Sandia National Laboratories, 1985.
[14] M. Berman, A critical review of recent large-scale experiments on hydrogen-air detonations, Nucl. Sci. Eng. 93 (1986) 321–347.
[15] R. Atkinson, D.C. Bull, P.J. Shuff, Initiation of spherical detonation in hydrogen/air, Combust. Flame 39 (1980) 287–295.
[16] C. Sadee, D.E. Samuels, T.P. O'brien, The characteristics of the explosion of cyclohexane at the HYPRO (UK) Flixborough plant on 1st June 1974, J. Occup. Hazards 1 (1977) 203–235.
[17] H. Siefert, H. Giesbrecht, Safer design of inflammable gas vents, Loss Prev. Safety Promotion 5 (1986) 70-1–70-21.
[18] B.J. Wiekema, Vapor cloud explosions—an analysis based on accidents, J. Hazard. Mater. 8 (1984) 295–311.
[19] A.C. van den Berg, The multi-energy method. A framework for vapor cloud explosion blast prediction, J. Hazard. Mater. 12 (1985) 1–10.
[20] M.J. Tang, Q.A. Baker, A new set of blast curves from vapor cloud explosion, Process Safety Progress 18 (1999) 235–240.
[21] B. Lewis, G. von Elbe, Combustion Flames and Explosions of Gases, Academic Press, New York, 1989, p. 388.
[22] R. Strehlow, Combustion Fundamentals, McGraw-Hill, New York, 1984.